Civil Engineering Infrastructures Journal 2025, 58(1): 103-121
DOI: 10.22059/ceij.2024.365637.1963

RESEARCH PAPER

Investigation of a Loaded Pile Responses Due to Proposed Deep Excavation in Sand Soil: Finite Element Analysis Using Plaxis3D Program

Hakeem, B.M.[1*]

[1] Associate Professor, Civil Engineering Department, Higher Institute of Engineering and Technology, New Minia, Egypt.

Received: 20 Sep. 2023; Revised: 16 Dec. 2023; Accepted: 14 Jan. 2024

ABSTRACT: Geotechnical design engineers are giving increasing attention to how piles respond to soil movements brought on by nearby braced excavations. This study investigates the effect of deep excavation on an adjacent loaded single pile on sand soil using the PLAXIS 3D finite element program. Leung et al. (2006) centrifuge test results were employed to verify the numerical model. The different parameters in this study were the excavation depth, type of pile head, diameter of pile, and the distance between the pile and the excavation. The results of the investigation demonstrated that the excavation depth (He) in proportion to the pile's length (Lp) has an important effect on pile responses. The case of (He/Lp = 2.0) leads a maximum lateral deflection at the pile toe of 24.80% from the diameter of pile. However, the lowest lateral deflection at the pile-0.85% of the pile diameter-occurs in the case where He/Lp = 0.5, which reduces. When He/Lp = 0.5, 1.0, the maximum value of bending moment of the pile occurs at around 0.70% normalized depth of the pile, or 230 and 298 kN.mm, respectively. Furthermore, the pile's response is greatly affected by the distance between it and the excavation site; after 10 meters, the value of bending moment in the pile is insignificant. Furthermore, it was found that while the maximum pile lateral deflection reduces as pile diameter increases, the bending moment along the pile remains constant. In this paper, the type of pile head was also discussed.

Keywords: PLAXIS 3D, Deep Excavation, Pile, Deflection, Bending Moment.

1. Introduction

Pile foundations are recommended when heavy structural loads have to be transferred from soil of lower-bearing capacity to a stratum of high bearing capacity. The influence of generated ground movement on the lateral response of an existing pile was investigated by Madhumathi and Ilamparuthi (2018) using 1 g model experiments on a single pile implanted in sandy soil. Depending on the pile's Lp/dp ratio, deflection reduces with spacing, and a decrease in deflection is noticeable for the shorter pile (Lp/dp = 10). Regardless of the placement of the pile, the deflection is less for piles with Lp/dp < 20. According to Zhang et al. (2018) the maximum values of the pile's lateral deflection and bending moment decrease noticeably as the pile gets farther away from the excavation edge.

Furthermore, the type of pile head greatly affects the pile's response, and an increase in axial force has a minimal impact

* Corresponding author E-mail: civileng_beshoy@mhiet.edu.eg

on the pile's behavior. Shakeel and Ng (2017) examined the behavior of a 2 × 2 pile group adjacent to a deep excavation in soft clay using a three-dimensional coupled consolidation analysis. Among the subjects covered were the effects of working load, soil permeability, pile length, pile group location from excavation, stiffness of the supporting system, and soil condition.

Ashour (2021) introduced research to study the value of bending moment, settlement, and lateral deflection of a loaded pile adjacent to a propped deep excavation using a Finite Element (FE) program. He concluded that the excavation depth behind the retaining wall considerably affects the ground surface settlement, and the settlement curve deepens as the excavation depth rises. Additionally, the ground movement increases significantly with increasing excavation depth and reduces noticeably with decreasing wall distance.

The ABAQUS program was utilized in a parametric analysis by Nishanthan et al. (2016) to investigate the pile responses caused by deep excavation in clay. They concluded that the stiffness, fixity, and distance of the pile head in the wall support system all significantly affected the behavior of the pile. Lateral movements in the surrounding soil are certain to occur as a result of stress reduction from the development of underground infrastructure and the excavation needed for basement construction adjacent to existing buildings.

It is necessary to consider both the buildings' safety and the stability of the foundations supporting them in this situation (Soomro et al., 2019). Li and Yang (2023) presented a study to examine the influence of pile groups to combined horizontal soil loading from excavation and surcharge. The results reveal that, in terms of pile group lateral displacement, capped-head pile groups can offer greater constraint than free-head pile groups. A 2-D finite element numerical model is used to examine the behavior of pile groups adjacent to deep sand excavations (Shafee and Fahimifar, 2018). The results show that excavation-induced alterations to adjacent pile groups can be accurately simulated using a basic 2-D plane strain model. They found that additional bending moments are imposed on piles as excavation depth is increased, and this should be taken into account while establishing the pile's structural design. Also, the result indicates that for pile groups adjacent to an excavation, incline loading causes additional lateral deformations and bending moments. Simultaneous vertical and horizontal loading, which primarily affects the upper half of piles, can result in severe lateral deformation, structural damage to piles, and serviceability issues.

In the study of Yi (2022), a three-dimensional Finite Difference Technique (FDM) was utilized to simulate a single pile that was exposed to loading of passive effect due to a new embankment in soil that was primarily composed of soft clay. He found that the lateral earth pressure at the pile increased with decreasing pile stiffness, while it increased with increasing embankment height and cushioning thickness. The behavior of a single pile behind a stable retaining wall in clay that is subjected to excavation-induced soil movements has been studied using a series of centrifuge model tests. The results show that the soil and wall continue to move even after the earth has been removed, causing the adjacent pile to bend and deflect (Leung et al., 2006). Additionally, once the excavation is complete, extra pore pressure is released, which eventually results in the wall and soil sliding.

Through extensive numerical parametric research, the interaction behavior between currently loaded piles and braced excavation design factors was examined in saturated sand (Shabban et al., 2023). They discovered that by raising the strut axial rigidity, the induced pile group settlement and tilting can be lessened because of the lowered soil motions during the excavation. A negligible difference in the pile group settling occurs as the wall embedded depth grows when the excavation depth is very

small. It has been found that reducing pile group tilting and settlement for deeper excavations can be achieved by increasing the wall penetration depth to excavation depth ratio.

According to Le and Nguyen (2021) an extensive excavation was done in the deep layer of soft soil in order to establish the basement floor and pile cap foundation for the 15-story skyscraper in Ho Chi Minh City. Due to the thick, weak soil (clay loam), a large embankment load (70 kN/m^2) far from the pit and a load from nearby construction and the construction machinery (10 kN/m^2) away from the excavation's side of 2.6 m caused a large displacement of bending moments inside the pile, which exceeded the pile's bending resistance moment and resulted in pile failure.

Soomro et al. (2020) stated that in order to estimate the deformation mechanism of a twenty-story building situated on a (4 × 4) piled raft to an adjacent twenty-five-meter-deep basement excavation, a 3D numerical parametric research was carried out. The excavation caused the raft to settle differently. The result was a persistent interstate drift in the 20-story skyscraper as it was displaced laterally towards the excavation. The building's structural components may experience strain due to interstate drift.

According to Shaban et al. (2023), there is a possibility that the adjacent piled buildings will tilt and settle as a result of varying levels of excavation for the new constructions. Accurately forecasting soil movement and pile response is critical to preventing damage to neighboring structures Finite Element numerical models are used to calculate the responses of the pile groups. The parametric research has changed pile group configurations, new building load, and center-to-center pile spacing. The groups of 2, 4, and 6 capped head piles next to excavation sites were all investigated.

Alielahi et al. (2014) assessed the effectiveness of under-reamed piles in clayey soils. Their research aimed to compare the performance of full and half bulbs under piles and conventional piles of the same length and volume in clayey soils. Using Plaxis 3D foundation software with a finite element base, bearing capacity diagrams were plotted for this purpose, and the outcomes were compared. Half-bulb under-reamed piles performed better than other piles, exhibiting reduced displacements, and higher compressive bearing capacities, according to analysis and computation results. Additionally, under piles demonstrated a smaller uplift and a higher ultimate tensile bearing capacity in comparison to conventional piles of the same length and different volume.

In the current study, the 3D PLAXIS finite element program will be employed to perform computational analyses in three dimensions in order to acquire new understanding of how piles respond to nearby deep excavation in sand. The most significant influences on pile response (i.e., excavation depth, type of pile head, pile diameter, and distance from pile to excavation) will be studied using the validated model. The value of bending moment, later deflection, and settlement of the pile will be considered the pile response in this research.

2. Using Centrifuge Test Results to Verify the Plaxis3D Finite Element Model

2.1. Current Study Objectives

The objectives of this study is:

a) Verifying the viability of the selected computational procedures by comparing the centrifuge test results obtained by Leung et al. (2006) with those obtained by the PLAXIS (3D) finite element model software.

b) To find out how a loaded pile responds in sand soil to a propped deep excavation.

c) The effect of excavation depth, type of pile head pile diameter, and distance

from pile to excavation on the influence of pile.

2.2. Centrifuge Model Setup (Leung et al., 2006)

Centrifuge Model of Leung et al. (2006) was used in this study. They used the centrifuge test to evaluate the 3D finite element numerical model employed in this parametric analysis. To investigate the behavior of the piles as a result of nearby soft clay excavation, a centrifuge test with 50 g centrifuge acceleration was conducted in the instance of a stable retaining wall.

The stainless steel model container's inside dimensions are 200 mm in width, 470 mm in height, and 540 mm in length. The container was first filled with 120 mm of Toyoura sand (in prototype scale equal to 6 m), and then with 130 mm of Malaysian kaolin clay (6.5 m in prototype scale). The wall model for the centrifuge test was a 3 mm thick aluminium plate, while the pile model was made from a hollow square aluminium tube. After the model of pile and wall were set in location, the clay layer in the excavation zone was carefully taken out and replaced with a latex bag filled with a solution of ZcCl2 that has the same density as the clay that was taken out. The centrifuge physical model established by Leung et al. (2006) is shown in Figure 1. The centrifuge model built at prototype scale by Leung et al. (2006) is shown in Figures 2 and 3 in cross section and a plane view, respectively.

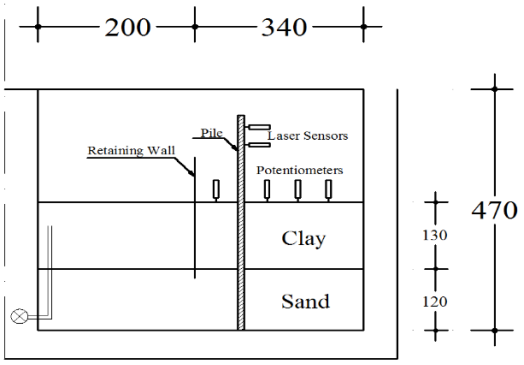

Fig. 1. Centrifuge model setup, all dimensions in mm (Leung et al., 2006)

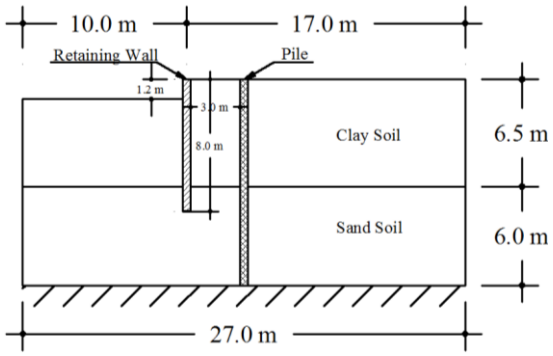

Fig. 2. Cross section of the prototype-scale centrifuge model (Leung et al., 2006)

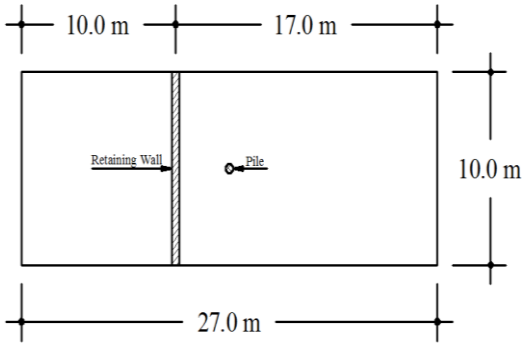

Fig. 3. Plane view of the prototype-scale centrifuge model (Leung et al., 2006)

2.3. Material Characteristics Used in Centrifugal Testing

Based on the Leung et al. (2006) the PLAXIS 3D program was employed to simulate the centrifuge test. The kaolin clay used in the centrifuge test was modelled using the Modify Cam Clay model (MCC), which has been used to investigate the behaviour of usually soft soils (PLAXIS 3D Material Models V21). In order to simulate the behaviour of the sand used in the centrifuge test, the Hardening Soil Model (HS) (PLAXIS 3D Material Models V21) was used. The kaolin clay, the sand parameters employed in the finite element study are listed in Tables 1 and 2 (Leung et al., 2006).

Using a hollow square aluminium tube, the pile model for the centrifuge test was constructed, a bending rigidity, EI of 2.2×10^5 kN.m^2. This value corresponds to a 600 mm diameter cast-in-situ Grade 35 concrete bored pile with a length of 12.5 m in prototype scale. The prototype bending moment for the model of retaining wall, which was made of a 3 mm thick aluminium plate, was 24×103 kN.m^2/m. The pile characteristics employed in the analysis are listed in Table 3.

2.4. Centrifuge Test Simulation in Three Dimensions Using Finite Elements

The centrifuge test was modelled in PLAXIS 3D at prototype scale (Figures 2 and 3). Because of the model's symmetry, only half of the model was simulated. The Modify Cam Clay model (MCC), which is appropriate for simulating the behaviour of usually consolidated soft soils, and the Hardening soil model were used for modelling the sand soil. The mesh size was determined to be 27, 10 and 12.5 m in the X, Y, and Z axes. The model's bottom side was restricted in all directions, but the model's vertical sides were restrained from moving in a horizontal manner. Any movement in the top half was possible. Using a 10-node element, the soil was simulated. Three-node line beam components were used to model the pile as an embedded beam.

Table 1. Geotechnical parameters of the kaolin clay that was used in this verification

Dry properties	Value	Unit	Reference
Unit weight (γ_{dry})	15.21	kN/m^3	
Coefficient of permeability (μ)	1.36×10^{-8}	m/s	
K_0 Value for normal consolidation (K_0^{nc})	0.60	-----	Leung et al. (2006)
Cam-clay compression index (λ)	0.64	-----	
Cam-clay swelling index (k)	0.14	-----	
Tangent of the critical state line (M)	0.90	-----	Teh et al. (2005)
Friction Internal Angle (Ø)	23	º	Leung et al. (2006)
Poisson's ratio (ν)	0.30	-----	Bowles (1997)

Table 2. Geotechnical parameters of the toyoura sand that was used in this verification

Properties	Value	Unit	Reference
Dry Unit weight (γ_{dry})	15.78	kN/m^3	
Triaxial compression stiffness (E_{50}^{ref})	30×10^3	kN/m^2	
Primary oedometer stiffness (E_{oed}^{ref})	24×10^3	kN/m^2	Nishanthan et al. (2016)
Unloading/reloading stiffness (E_{ur}^{ref})	99×10^3	kN/m^2	
K_0 value for normal consolidation (K_0^{nc})	0.318	-----	
Reference stress for stiffness (p^{ref})	100	kN/m^2	
Friction Internal Angle (Ø)	43	º	Leung et al. (2006)
Dilatancy angle (ψ)	15	º	
Poisson's ratio (ν)	0.30	-----	Bowles (1997)

Table 3. Geotechnical parameters of the pile that was used in this verification

Properties	Value	Unit	Reference
Bending rigidity (EI)	2.2×10^5	kN.m^2	Nishanthan et al. (2016)
Diameter	0.6	m	
Length	12.5	m	

A specific interface element explained the interaction between the earth surrounding the foot and skin of the pile. To represent the real contact between the soil and the wall, a 12-node interface element was used. The default mesh refinements value was utilized to refine the soil surrounding the elements. The wall was modelled as a triangular plate element with six nodes. As shown in Figure 4, the mesh was constructed of 12770 nodes and 7017 soil elements.

2.5. Comparison Between Experimental and Theoretical Results

Figures 5 and 6 show the generated bending moment as a result of the adjacent excavation and the computed and experimental lateral deflection profile along the pile. It was found from both measuring and numerical analysis that the pile head suffers the greatest lateral deflection. However, because of the pile's free head, the induced Bending Moment (BM) was zero in both the computed and observed measurement. The numerical and experimental results were found to be in very good agreement, having a maximum difference as shown in Figures 5 and 6.

The results of the centrifuge test revealed the same trend for the lateral deflection and bending moments. In general, there is high agreement between the computed and measured results, as shown in Figures 5 and 6.

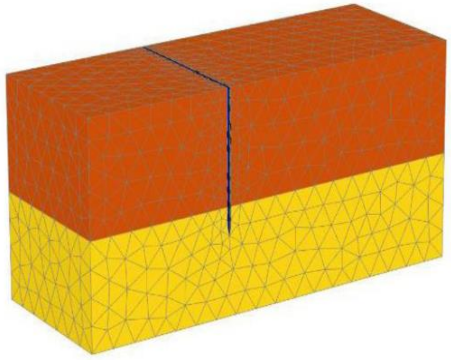

Fig. 4. 3D view of the used finite element mesh in modelling the centrifuge test

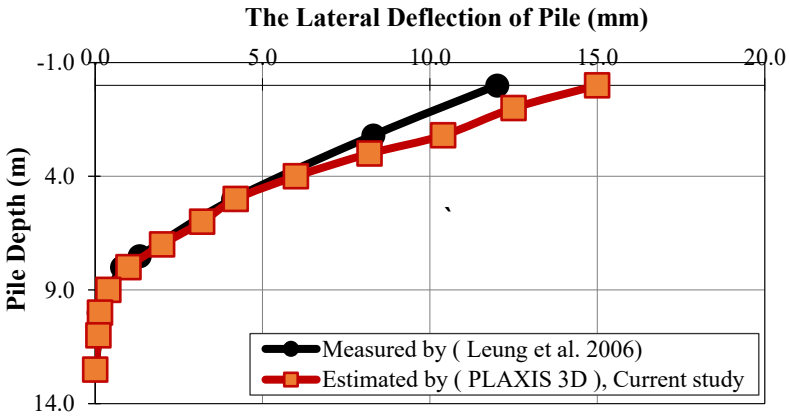

Fig. 5. Comparison of experimental and numerical induced lateral deflection along the pile length

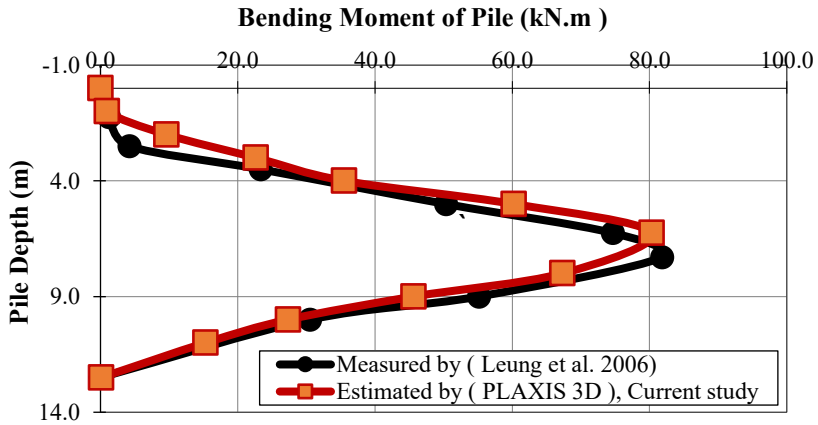

Fig. 6. Comparison of experimental and numerical induced bending moment along the pile length

Therefore, it can be used in the finite element analysis (PLAXIS 3D) that follows in this investigation.

3. Estimation the Bearing Capacity of Pile

Using the PLAXIS 3D program, a loaded pile test was carried out to determine the pile bearing capacity. A point load was applied gradually to a single bored concrete pile with a diameter of one meter, a length of twenty meters, and a modulus of elasticity of 30 GPa (with increments of 500 kN). The model's dimensions were chosen to be 40 × 40 × 40 m in the X, Y, and Z axes, respectively. The boundary condition effect was prevented by the larger dimensions in the same way as Nishanthan et al. (2016). Sand parameters are listed in Table 2, which was used to model the sandy soil. In this study, the pile was embodied in the simulation by an embedded 3-node line element. The curve for load-settlement is shown in Figure 7. Using the settlement-based failure criterion for large-diameter piles provided by Ng (2001), the pile's ultimate capacity was calculated. Eq. (1) provides the failure criterion.

$$\Delta_{ph.max} \cong 0.045\, d_p + \frac{1}{2}\frac{P_h\ L_p}{A_p E_p} \quad (1)$$

where d_p: is the diameter of pile, P_h: is the load placed on pile, L_p: is the pile length, A_p: is the pile area, E_p: is modulus of elasticity of pile, $\Delta_{ph,\ max}$: is maximum head settlement at the ultimate capacity of the pile. Based on this equation, the ultimate value of pile bearing capacity was estimated to be about 5000 kN, and the working load was determined to be 1600 kN tacking a factor of safety of 3.

4. Numerical Modelling Using PLAXIS 3D

4.1. Geometry of the 3D Problem

A typical three dimensional finite elements numerical model was employed to carry out the parametric investigation, as shown in Figure 8.

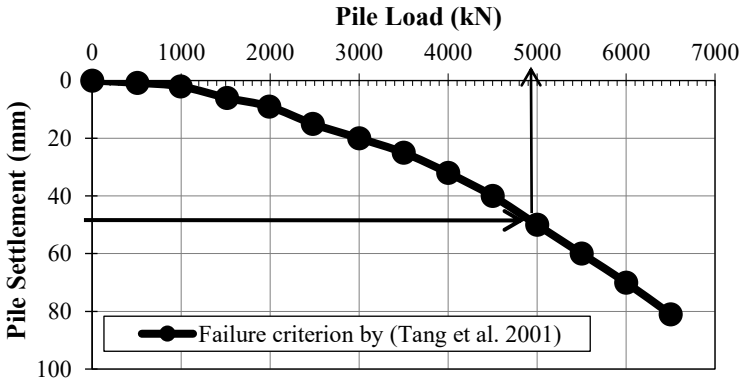

Fig. 7. Load versus settlement curve estimated by PLAXIS 3D program

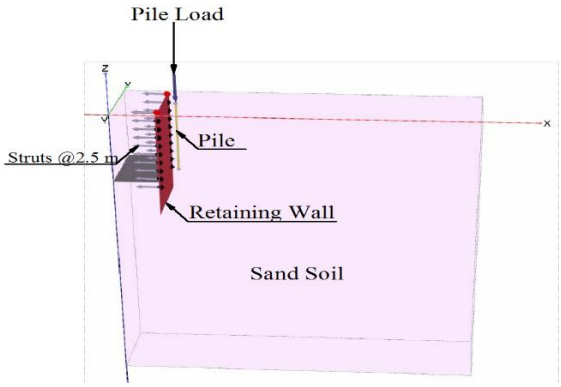

Fig. 8. Typical used finite element model

The dimensions of the model were determined to be 60, 20 and 80 m in the X, Y, and Z axes, respectively. According to Nishanthan et al. (2016) these dimensions were adequate to avoid boundary conditions from having an effect.

4.2. Boundary Conditions

The model's boundary conditions were identical to those used in centrifuge test modelling, as shown in Figure 9. In the analysis, medium-type mesh was employed. The mesh that was used for the analysis as shown in Figure 10.

4.3. Different Parameters Used in This Study

The models used for these analyses with various He/Lp conditions are shown in Figures 11 to 14. In each analysis condition, the depth of retaining wall to excavation depth ratio was 1.5 in the same way as in (Hsiung, 2009). The length of pile was kept constant at twenty meters. An embedded beam was used to model the pile.

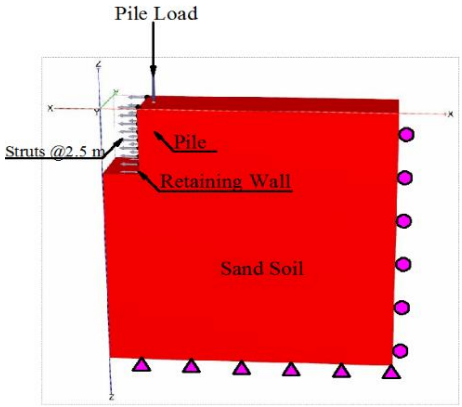

Fig. 9. Boundary conditions used in finite element model

Fig. 10. Finite element mesh

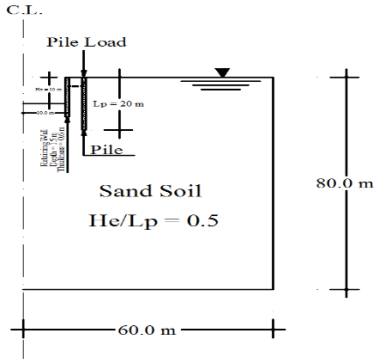

Fig. 11. Cross section of 3D model for (He/Lp = 0.5) case

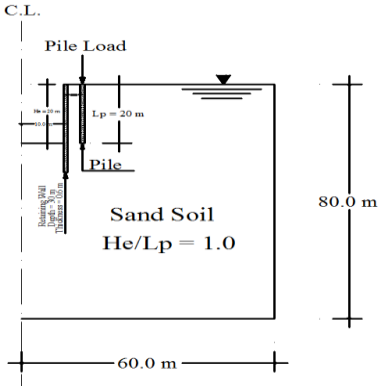

Fig. 12. Cross section of 3D model for (He/Lp = 1.0)

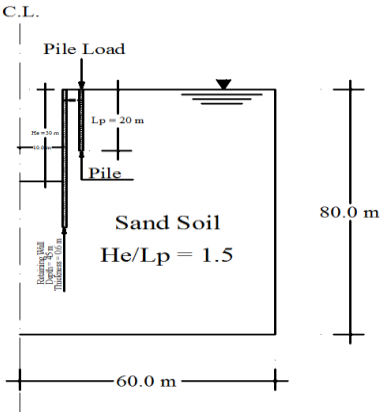

Fig. 13. Cross section of 3D model for (He/Lp = 1.5) case

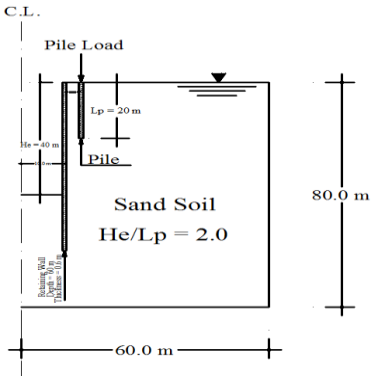

Fig. 14. Cross section of 3D model for (He/Lp = 2.0) case

Table 4 summarizes all the parameters taken into consideration in the present study. The program's flexible graphical interfaces make it simple for users to create a geometry model. The user interface consists of two subprograms: the input and output programs (PLAXIS 3D Reference Manual, 2020). Joint pieces called interfaces are used to simulate how soil and structure interact.

In order to approximate the area where a plate connects with the surrounding soil, they can also be formed adjacent to a plate, between two soil volumes, or between geogrid elements.

4.4. Material Models Parameters

Hardening Soil model (HS) was used for modeling the sand. Table 5 lists the sand characteristics that were used in the analysis. The characteristics of the sand were taken from the research of Unsever (2015). It was supposed that the groundwater table was at the surface in the same way as Nishanthan et al. (2016). In the vertical and horizontal planes, the struts were separated at 2.5 and 10 m, respectively. The pile properties are listed in Table 6.

Table 4. All cases have been studied in this research

Excavation depth, (He) (m)	He/Lp	Distance from the pile to the excavation, (X), (m)	Pile head type	Pile dia. (m)
10	0.5	3.0 = 15 % (He)	Free	0.5
20	1.0	5.0 = 25 % (He)	Hinged	1.0
30	1.5	10.0 = 50 % (He)	Rigid	1.5
40	2.0	20.0 = 100 % (He)		

Table 5. Geotechnical properties of the sand that was used in this study (Unsever, 2015)

Properties	Value	Unit
Dry unit weight (γ_{dry})	14.52	kN/m^3
Saturated unit weight (γ_{sat})	19.00	kN/m^3
Relative density (D_r)	70	%
Initial void ratio (e_{inital})	0.83	-----
Triaxial compression stiffness (E_{50}^{ref})	29.56 × 10^3	kN/m^2
Primary oedometer stiffness (E_{oed}^{ref})	24.65 × 10^3	kN/m^2
Unloading/reloading stiffness (E_{ur}^{ref})	99.59 × 10^3	kN/m^2
K_0 value for normal consolidation (K_0^{nc})	0.318	-----
Reference stress for stiffness (p^{ref})	100	kN/m^2
Cohesion (C)	0.1	kN/m^2
Friction internal angle (Ø)	43	º
Dilatancy angle (ψ)	15.8	º
Poisson's ratio (ν)	0.19	-----
Interface reduction factor	0.75	-----

Table 6. Geotechnical properties of the embedded pile that was used in this study (Unsever, 2021)

Properties	Value	Unit
Dry unit weight (γ_{dry})	25	kN/m^3
Young's modulus (E)	30 × 10^6	kN/m^2
Pile length (Lp)	20	m
Skin resistance	Layer dependent	-----
Max. skin resistance (T_{max})	380	kN/m^2
Max. base resistance (F_{max})	1598	kN/m^2

Table 7. Geotechnical properties of the diaphragm wall was used in this study (Unsever, 2021)

Properties	Value	Unit
Dry unit weight (γ_{dry})	25	kN/m^3
Young's modulus (E)	30 × 10^6	kN/m^2
Poisson's ratio (ν)	0.3	-----
Thickness	0.6	m

Table 8. Geotechnical properties of the strut (fixed end anchor) was used in this study (Unsever, 2021)

Properties	Value	Unit
Axial rigidity	374.85×10^3	-----
Area	17.85×10^{-4}	m^2
Young's modulus (E)	210×10^6	kN/m^2

The values used for the bearing capacity characteristics are based on the research of Nishanthan et al. (2016). The analysis's diaphragm walls and strut parameters are displayed in Tables 7 and 8, respectively. Based on the failure criterion, a working load of 1600 kN was applied to the pile head.

4.5. The Standard Model Follows the Steps of Finite Element Modelling

The process of using finite elements can be outlines as follows:

- Soil model: Soil stratigraphy and the geometry model were created. Additionally, a data set for soil layers was developed.
- Structure model: All structural components, including the levels of excavation, the pile, the diaphragm walls, the loads, and the struts, were created. Next, it is necessary to define each element's structural characteristics.
- Mesh mode: A mesh has been created.
- Flow conditions: The groundwater level was assigned in this step.
- Staged construction: In this step, the building phases were specified as follow:
- Initial phase: It is a stage that PLAXIS automatically generates to start the initial stresses.
- Stage 1 Pile Construction: A 20 m long pile is constructed in this stage.
- Stage 2 Applying the load: At the pile's head, a load of 1600 kN was applied.
- Stage 3 Wall Construction: This stage included the installation of the diaphragm wall.
- Stage 4 Excavation: The top 2.5 m of earth have been excavated (deactivated).
- Stage 5 Strut Installation: The strut installation until reaching the final depth of excavation.

5. Results and Discussion

5.1. Effect of the Depth of Excavation on the Pile Response

To examine the influence of the depth excavation on the response of pile, four various case studies of excavation depth to a constant value of the pile length (i.e., 20 m) were studied. The excavation above, and below the pile toe is illustrated by these cases (He / Lp = 0.5, 1.0, 1.5 and 2).

5.1.1. The Induced Settlement Along the Length of Pile Due to the Excavation

Figure 15 illustrates how excavation causes the loaded pile to settle along its length in four different cases of (He/Lp).

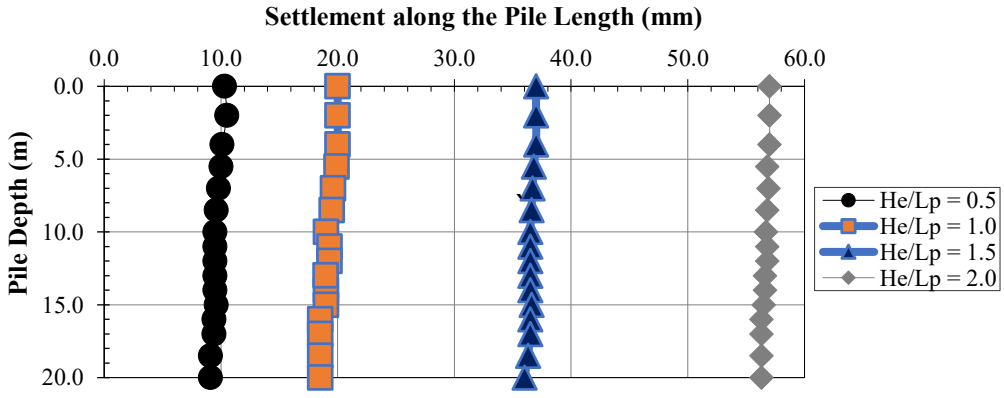

Fig. 15. The induced settlement along the pile length due to the excavation in four cases of (He/Lp)

Results indicate that as excavation depth increases, pile settlement also increases. Settlement is constant along the pile's axis. For the cases of (He/Lp = 0.5, 1, 1.5 and 2.0, respectively), the maximum pile settlement is 1, 2, 3.7, and 5.7% from pile diameter (= 1.0 m). This occurs due to the decrease in frictional resistance as the He/Lp increases, causing an increase in the settlement value.

5.1.2. The Lateral Deflection Induced Along the Length of Pile Due to the Excavation

The lateral deflection profile of the pile as a result of the excavation is shown in Figure 16 for four case of (He/Le). The pile is moving in the direction of excavation if the values are negative. The results indicate that in four different cases of (He/Lp), the pile deflected towards the excavation side, as would be predicted given that excavation causes soil to be displaced in that direction and reduces stress. When He/Lp = 0.5, the maximum lateral deflection value is 8.5 mm, (0.85% of the pile diameter), at the pile head, then the deflection decrease until 12 m of the pile length.

As shown in Figure 17, the lateral deflection value increases from the pile head and reaches a maximum value of 12.7 mm (1.27% of the pile diameter) at 11.0 m of the pile length. After that, the deflection starts to decrease according to the case of (He/Lp = 1.0). The pile toe shows the largest lateral displacement when He/Lp = 1.5, reaching a maximum of 22.7 mm (22.75% from the pile diameter).

Additionally, in the case of (He/Lp = 2.0), the pile toe experiences the greatest lateral displacement, which reaches a maximum of 24.8 mm (24.80 % of the pile diameter). It means that when He/Lp = 2.0, the pile toe obtains the most lateral deflection. While the pile toe experiences the lowest lateral deflection when He/Lp = 0.5. In addition, whereas pile toe lateral displacements are dependent on excavation depth, head of pile settlements are similar in all four cases. The reason for the increase in lateral deflection is that by increasing the excavation depth, and the pile is loaded, it causes movement in the direction of the excavation due to the lack of soil surrounding the pile, causing a decrease in its bearing capacity.

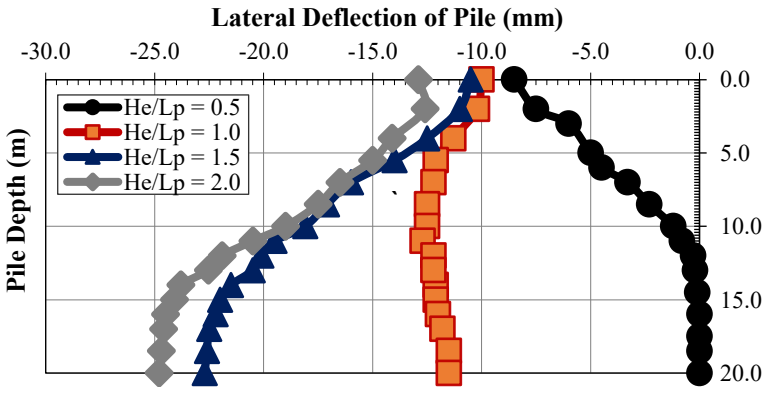

Fig. 16. The induced lateral deflection profile along the pile length due to the excavation in four cases of (He/Lp)

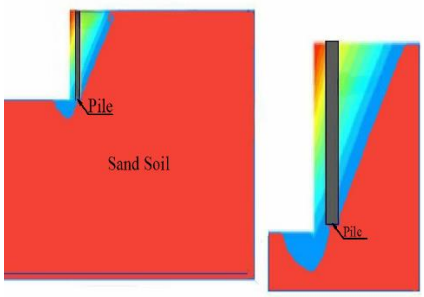

Fig. 17. The induced lateral deflection profile along the pile length. (He/Lp = 1.0)

5.1.3. Bending Moment Induced by Excavation Along the Pile Length

Figure 18 shows the generated bending moment profile at the pile as a result of the excavation in each of the four cases of (He/Lp). The pile is under tensile stress, which is toward the excavation, as illustrated by the negative values. The generated value of bending moment at the pile head is zero in all cases because of the pile's free head. According to the results, the upper length of the pile is where the negative bending moment always develops gradually. For case of (He/Lp = 0.5), the value of bending moment becomes positive in the portion below and then gradually decreases until the pile-toe bending moment, where it finally becomes zero. A similar bending moment behaviour exhibits for cases (He/Lp = 1, 1.5, and 2.0), where the full pile shaft experienced a negative bending moment, putting the pile shaft under tensile stress, and where the bending moment was zero at the pile toe. In all four cases, the maximum bending moment (positive or negative, depending on the excavation depth) occurs at a depth of roughly 0.70% of the normalized depth of the pile. For case of (He/Lp = 1), the pile toe was at the same level as the ultimate excavation depth, resulting in the highest moment. In contrast, for case of He/Lp = 0.5 produced a greater bending moment than the case of (He/Lp = 2.0) because the lower portion of the pile in the case of (He/Lp = 0.5) was subjected to higher levels of soil constrain. As a result, it may be said that the pile experiences the greatest bending moment when He/Lp = 1, and the least amount of bending moment when He/Lp = 2.0.

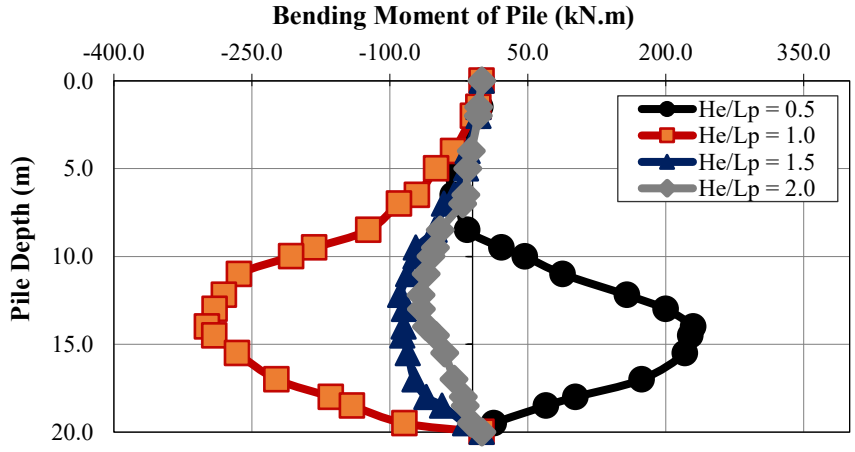

Fig. 18. The induced bending moment profile along the pile length due to the excavation in four cases of (He/Lp)

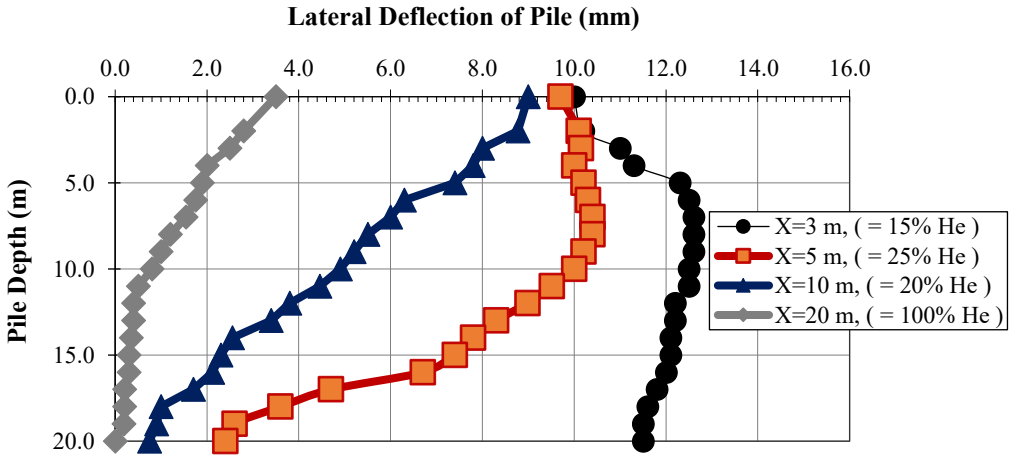

Fig. 19. Lateral deflection of the pile due to changing the distance from the pile to the excavation site (He/Lp = 1.0, He = 20 m)

5.2. The Influence of Excavation's Distance from the Pile on the Response of the Pile

The effect of the horizontal distance of the excavation site on pile reaction was investigated at four different distances: 5, 10, and 20 m (i.e., 15%, 25%, 50%, and 100% from the final excavation depth He). 20 m (He/Lp = 1) was the final excavation depth and pile length that kept constant. The results indicate that, as expected, the pile's lateral deflection decreases as the distance from the excavation (X) to the pile increases (see Figure 19). Additionally, it is obvious that, at a distance of 20 m, the value of lateral deflection of the pile head decreases significantly. In addition, the deflection of pile-toe decrease as the distance increases.

Furthermore, the bending moment along the pile length is clearly reduced as the distance from the pile to the excavation (X) increases, as shown in Figure 20. After a distance of 10 m between the excavation and the pile, it is found that the generated bending moments on the pile are neglected.

5.3. Influence of the Type of Pile Head on the Response of the Pile

The value of a pile's lateral deflection as a result of excavation for free, hinged, and rigid pile heads (He/Lp = 0.5, 1, 1.5, and 2.0, respectively) is shown in Figures 21 to 24. The hinged head indicates a pile group connected to a beam, whereas the stiff head represents piles restrained back by a rigid raft. The figures show that, in each of the three conditions, the deflection at the pile head was exactly zero due to the stiff head.

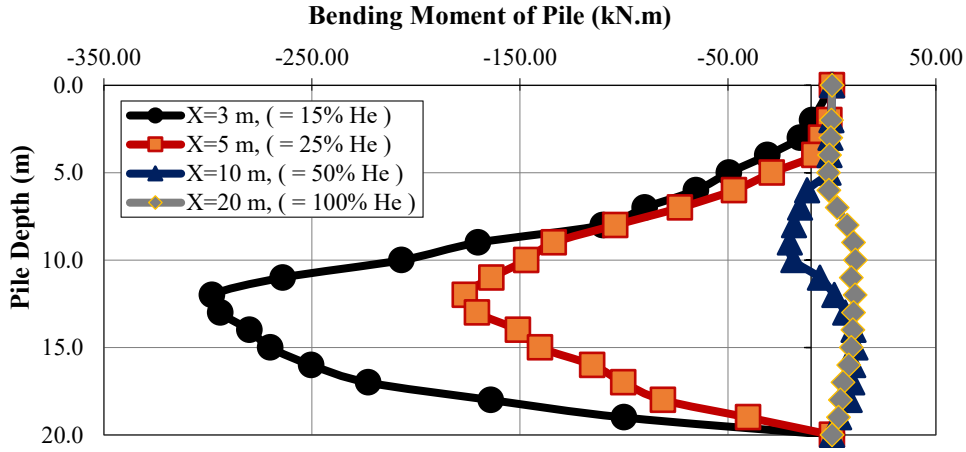

Fig. 20. Bending moment of the pile due to changing the distance from the pile to the excavation site (He/Lp = 1.0, He = 20 m)

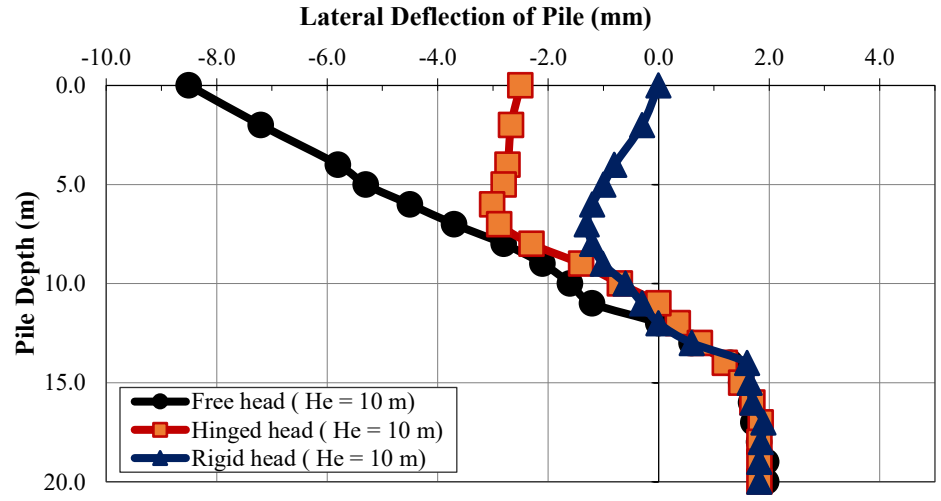

Fig. 21. Lateral deflection of the pile in case of free, hinged, and rigid pile head (He/Lp = 0.5)

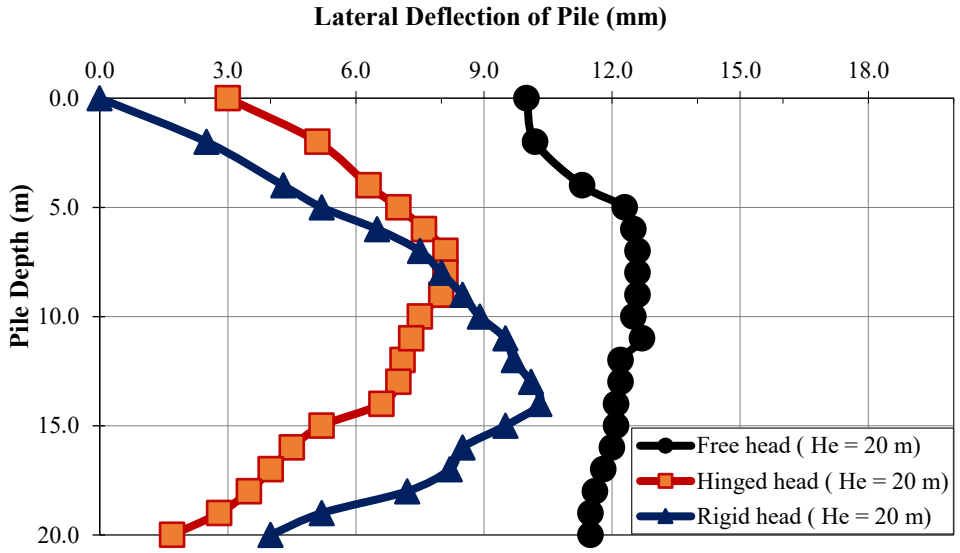

Fig. 22. Lateral deflection of the pile in case of free, hinged, and rigid pile head (He/Lp = 1.0)

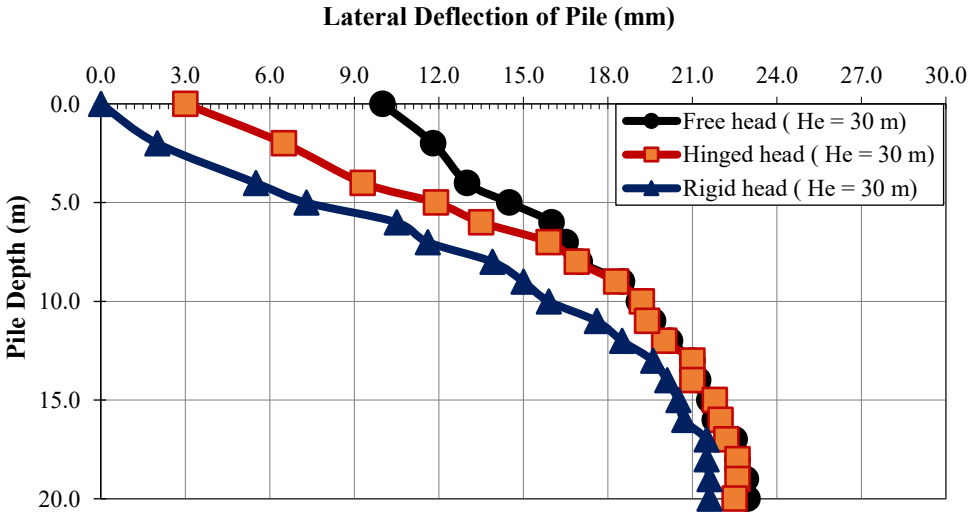

Fig. 23. Lateral deflection of the pile in case of free, hinged, and rigid pile head (He/Lp = 1.5)

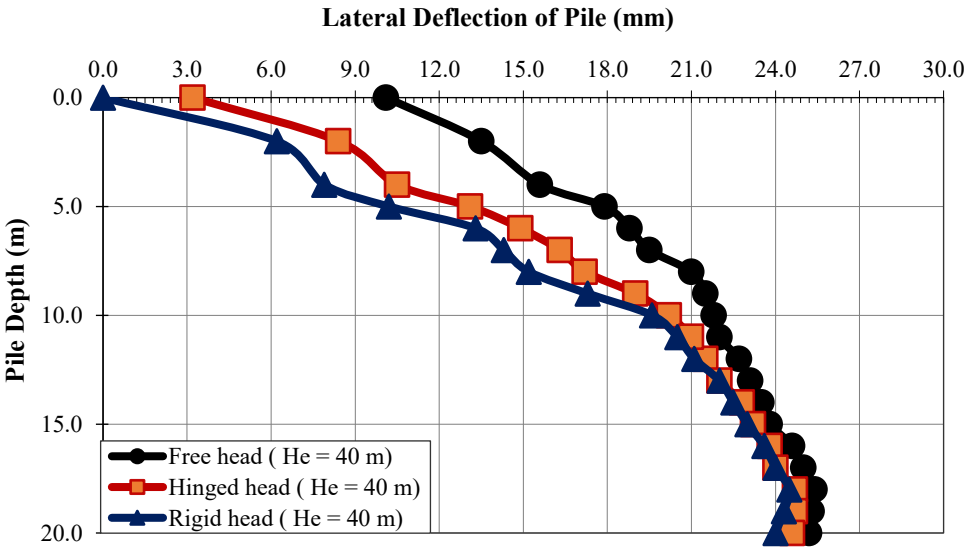

Fig. 24. Lateral deflection of the pile in case of free, hinged, and rigid pile head (He/Lp = 2.0)

This is due to the pile head's restrictions against both horizontal and vertical movement. Additionally, it should be mentioned that the maximum deflection for (He/Lp = 1.5) was about at the pile's mid-depth, but for (He/Lp = 2.0) the highest deflection for all pile head conditions was near the pile's toe. The generated pile bending moment for free, hinged, and rigid pile heads, respectively, are shown in Figures 25 to 28 for each of the four cases of (He/Lp = 0.5,1,1.5 and 2.0).

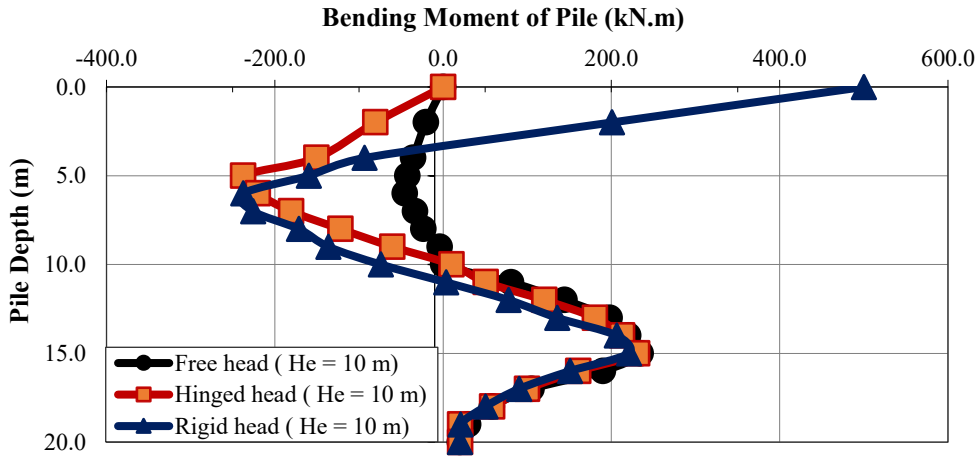

Fig. 25. Bending moment induced along the pile length in case of free, hinged, and rigid pile head (He/Lp = 0.5)

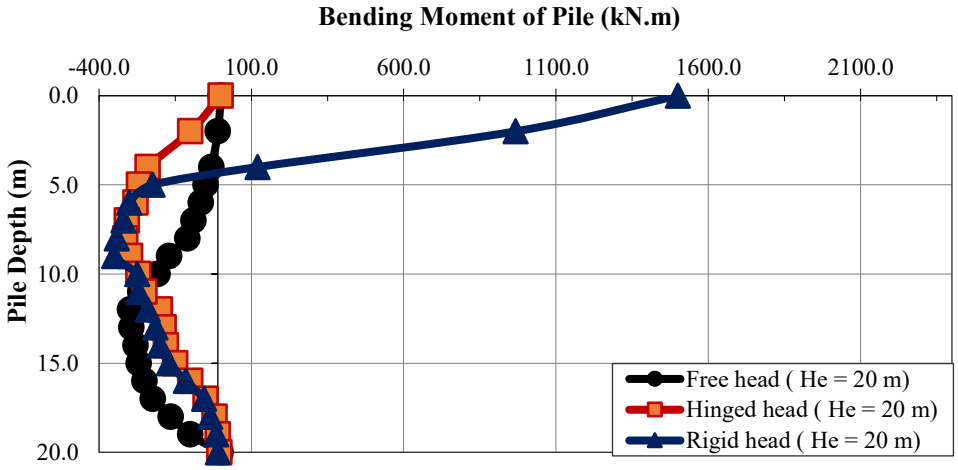

Fig. 26. Bending moment induced along the pile length in case of free, hinged, and rigid pile head (He/Lp = 1.0)

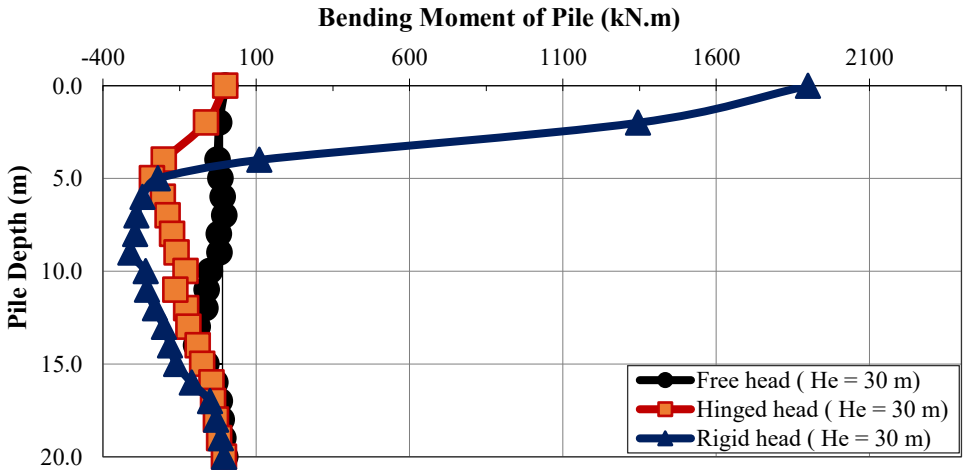

Fig. 27. Bending moment induced along the pile length in case of free, hinged, and rigid pile head (He/Lp = 1.5)

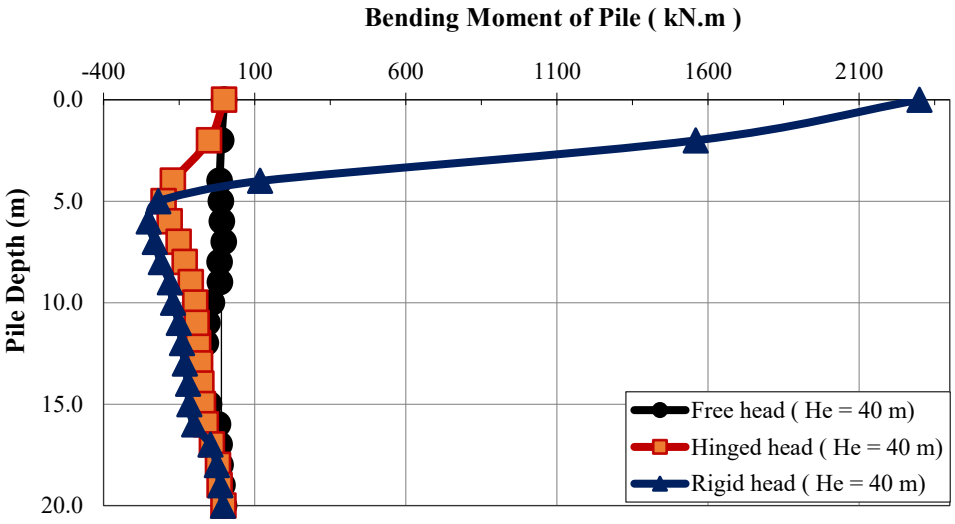

Fig. 28. Bending moment induced along the pile length in case of free, hinged, and rigid pile head (He/Lp = 2.0)

If the values are negative, there is tensile stress on the pile along its shaft. At the pile head, a significant positive bending moment was created because the movement of the pile head was restricted in the case of a rigid head. Figures 25 to 28 show how the generated positive BM at the pile head grows with increased excavation depth. Consequently, it might be considered that the type of pile head and the depth of the excavation have a significant role in determining how the pile responds to excavation, especially when the pile head is rigid and induces a substantial positive bending moment.

5.4. Effect of the Pile Diameter on the Pile's Response

Three varied diameters of 0.5, 1.0, and 1.5 m were investigated to examine the impact of pile diameter on the pile reaction. The excavation was limited to a depth of 20 m, and the pile length was kept at 20 m throughout these analyses. The lateral deflection of the pile due to variations in the pile's diameter is shown in Figure 29. For the case of (He/Lp = 1.0), the maximum values of lateral deflection are 1.05%, 1.27% and 3.16% from pile diameter, respectively.

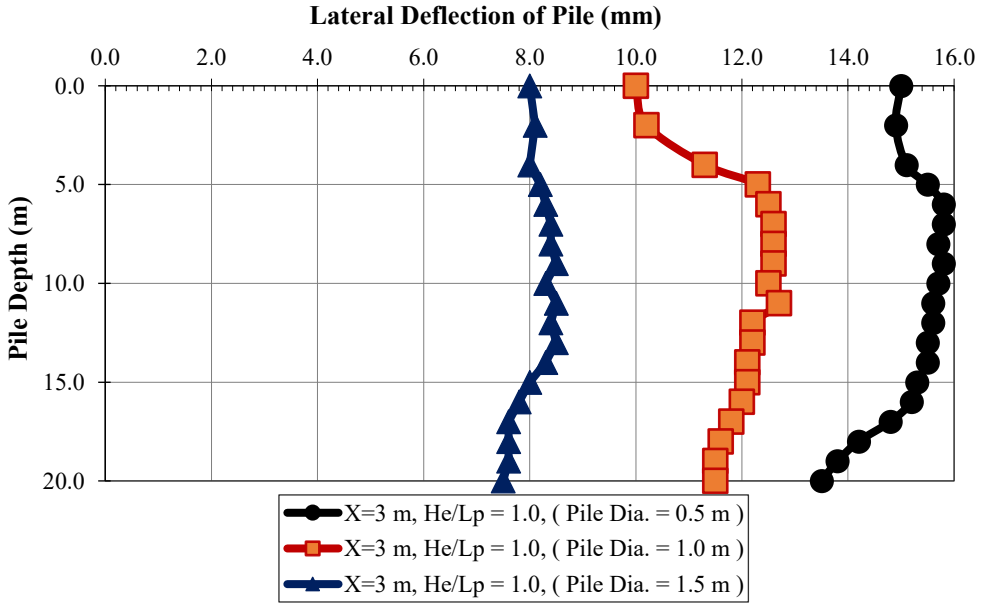

Fig. 29. Lateral deflection of the pile due to changing the pile diameter (He/Lp = 1.0)

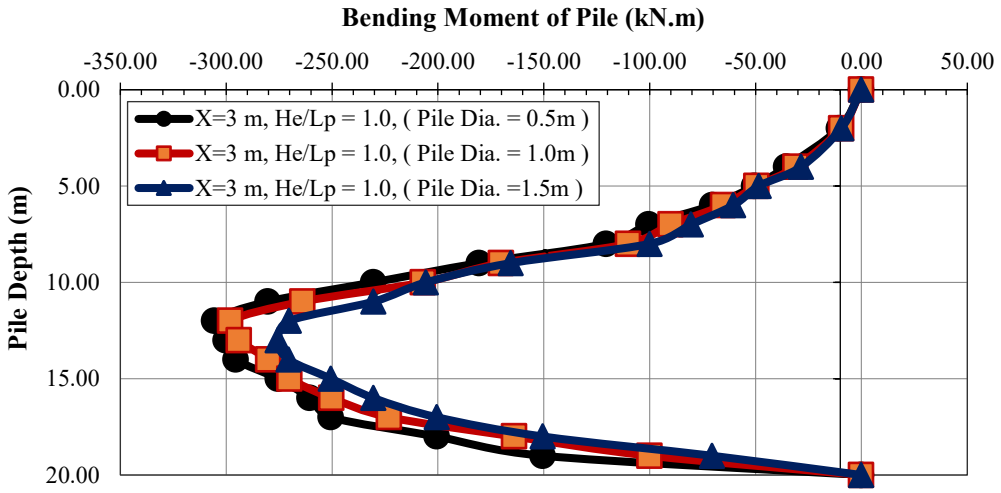

Fig. 30. The induced bending moment of the pile due to changing the pile diameter (He/Lp = 1.0)

Additionally, Figure 30 shows how the pile's bending moment changed as the pile's diameter increased. As a result, the results show that there are no appreciable differences between the three pile diameter scenarios. The results show that with increasing pile diameter, there is a decrease in the value of lateral deflection of the pile due to the increase in the contact area between the pile and surrounding soil; hence, the bearing capacity of the pile increases and there is a decrease in lateral deflection.

6. Conclusions

Using PLAXIS 3D software, a 3D finite element analysis was carried out in the present study to investigate how nearby deep excavation affected the behaviour of a loaded single pile in sand soil. A parametric study was carried out to determine the effect of different factors on pile behaviour, such as excavation depth, distance from pile to excavation site, pile head type, and diameter pile (after Leung et al., 2006), once the finite element model had been validated using previously presented centrifuge test results. Based on the results of the finite element analysis, the followings are the study's recommended conclusions:

- The maximum pile settlement for each case of He/Lp = 0.5, 1, 1.5 and 2.0 is 10, 20, 37 and 57 mm, or 1, 2, 3.7 and 5.7% from the diameter of pile (= 1.0 m).
- The pile toe is where the largest lateral deflection occurs when He/Lp = 2.0, whereas the pile toe is where the lowest lateral deflection occurs when He/Lp = 0.5.
- The maximum magnitude of the bending moment occurs at roughly 0.70% of the normalized depth of the pile. When the pile toe and the final excavation depth were at the same level, the maximum moment was generated for He/Lp = 1. As a result of increased soil restraint on the lowest part of the pile for He/Lp = 0.5 the bending moment in that scenario was larger than He/Lp = 2.0 case.
- The lateral displacement of the pile significantly reduces with increasing distance from the excavation site (X). However, the bending moments in the pile become negligible at ten meters of distance between the excavation and the pile.
- A significant factor influencing the behaviour of the pile is the type of pile head. If the head of the pile is rigid, a large positive moment is created at the pile head. Therefore, it can be summarized that the type of pile head and the depth of the excavation have a major effect on the pile's response during excavation, particularly in the case of rigid pile heads where a strong positive value of bending moment is induced at the pile head.
- Additionally, the maximum deflection for He/Lp = 1.5 was about at the pile's mid-depth, but for He/Lp = 2.0 the highest deflection for all pile head conditions was

near the pile's toe.
- As pile diameter increases, the maximum pile lateral deflection decreases.
- Increased pile diameter has no effect on the pile's bending moment.
- Thus, it can be concluded that if the most important safety measures are not followed. Depending on the length and depth of the excavation as well as the characteristics of the soil and pile, a new excavation site can significantly alter the stability of the present pile structure.
- As a limitation, this study focused on the single pile, the pile subjected to axial force only, no bending moment allowed.

7. Suggestions for Future Studies

The following cases are possible for conducting research:
- PLAXIS 3D can be used for the study to examine how adjacent pile groups subjected to inclined loading are affected by deep excavation.
- In the present study, PLAXIS 3D was used to analyse how a single pile developed as a result of adjacent deep excavation. It is suggested to simulate such cases in future research using programs such ABAQUS, Midas, and Flac.
- To examine how pile group behaviour connected by a raft foundation is affected by deep excavation.
- The provision of high diaphragm wall thickness or high supporting system stiffness would influence all results, therefore this should be taken into account.
- Studying the effect of ground water table in this analysis.

8. Notations

A: The pile area
BM: Bending moment
D_r: Relative Density
EI: Bending rigidity
E: The elastic modulus of the pile
e_{inital}: Initial void ratio
E_{50}^{ref}: Triaxial compression stiffness
E_{oed}^{ref} : Primary oedometer stiffness
E_{ur}^{ref} : Unloading/reloading stiffness
FE: Finite element
F_{max}: The maximum base resistance
He: Final depth of excavation
HS: Hardening soil model
He/Lp: Excavation depth to pile length ratio
k: Cam-clay swelling index
Lp: Pile length
Lp/dp: Pile length to pile diameter ratio
LD: Lateral deflection
M: Tangent of the critical state line
MCC: Modify Cam Clay
T_{max}: Maximum skin resistance
X: Distance from the excavation to the pile (center to center)
γ_{dry}: Soil unit weight
γ_{sat}: Saturated unit weight
μ: Coefficient of permeability
K_0^{nc}: Value for normal consolidation
λ: Cam-clay compression index
Ø: Friction Internal Angle
ν: Poisson's ratio
p^{ref}: Reference stress for stiffness
ψ: Dilatancy angle
$\Delta ph,max$: Maximum pile head settlement at the pile ultimate capacity

9. References

Alielahi, H., Mardani, Z. and Daneshvar, S. (2014). "Influence of under-reamed pile groups arrangement on tensile bearing capacity using fe method", *Electronically Journal of Geotechnical Engineering (EJGE)*, 19, 1395-1410, https://www.researchgate.net/publication/271445649.

Ashour, S. (2021). "Analyses of the effect of deep excavation on behaviour of adjacent pile in sand using 3d finite element method", MSc. Thesis, Bursa Uludağ University, http://hdl.handle.net/11452/22363.

Bowles, J.E. (1997). *Foundation analysis and design*, The McGraw-Hill Companies, Inc., Fifth Edition, ISBN 0-07-912247-7, https://apilibrary.lqdtu.edu.vn/media/FoundationAnalysisAndDesign.pdf.

Hsiung, B.C. (2009). "A case study on the behaviour of a deep excavation in sand", *Computers and Geotechnics*, 36(4), 665-675, https://doi:10.1016/j.compgeo.2008.10.003.

Leung, C.E., Ong, D.E. and Chow, Y.K. (2006). "Pile behaviour due to excavation-induced soil movement in clay. i: stable wall", *Journal of*

Geotechnical and Geoenvironmental Engineering, 132(1), 36-44, https://doi:10.1061/(ASCE)1090-0241(2006)132:1(36).

Le, N.T. and Nguyen, T.A. (2021). "3D finite element analysis of pile behaviour inside the deep excavation in soft soil", *International Journal of Engineering Research and Technology (IJERT),* 10(1), 5-10, http://doi.org/10.17577/IJERTV10IS010007.

Li, T. and Yang, M. (2023). "Investigation of passive pile groups' responses induced by combined surcharge-induced and excavation-induced horizontal soil loading", *Buildings*, 13(11), 2775, 1-13, https://doi.org/10.3390/buildings13112775.

Madhumathi, R.K. and Ilamparuthi, K. (2018). "Laboratory study on response of single pile adjacent to supported cut", Geotechnical and Geological Engineering, 36, 3111-3133, https://doi.org/10.1007/s10706-018-0524-9.

Nishanthan, R., Liyanapathirana, D.S. and Leo, J. (2016). "Shielding effect in pile groups adjacent to deep unbraced and braced excavations", *International Journal of Geotechnical Engineering*, 11(2), 162-174, https://doi.org/10.1080/19386362.2016.1200270.

Ng, C.W., Yau, T.L., Li, J.H. and Tang, W.H. (2001). "New failure load criterion for large diameter bored piles in weathered geomaterials", *Journal of Geotechnical and Geoenvironmental Engineering*, 127(6), 488-498, https://doi.org/10.1061/(ASCE)1090-0241(2001)127:6(488).

PLAXIS 3D-Reference Manual. (2020). "CONNECT Edition V20.03", Bentley, June, https://www.scribd.com/document/516563012/FEM-2D-Reference.

Shafee, A. and Fahimifar, A. (2018). "Numerical investigation on the effects of deep excavation on adjacent pile groups subjected to inclined loading", *International Journal of Geotechnical and Geological Engineering*, 12(7), 489-49, https://www.scribd.com/document/707142821/10009284.

Shakeel, M. and Ng, C.W. (2017). "Settlement and load transfer mechanism of a pile group adjacent to a deep excavation in soft clay", *Computers and Geotechnics*, 96, 55-72, http://doi.org/10.1016/j.compgeo.2017.10.010.

Shabban, M.G., Abd El-Naiem, M.A., Senoon, A.A. and Kenawi, M.A. (2023). "Interaction analysis between existing loaded piles and braced excavation design parameters", *Journal of Engineering Sciences (JES)*, 51(3), 189-206, https://doi.org/10.21608/jesaun.2023.187262.1199.

Shabban, M.G., Abd El-Naiem, M.A., Senoon, A.A. and Kenawi, M.A. (2023). "Effects of excavation and construction sequence on behaviour of existing pile groups", *Innovative Infrastructure Solutions*, 8(223), 1-12, https://doi.org/10.1007/s41062-023-01193-8.

Soomro, M.A., Mangnejo, D.A., Bhanbhro, R., Memon, N.A. and Memon, M.A. (2019). "3D finite element analysis of pile responses to adjacent excavation in soft clay: Effects of different excavation depths systems relative to a floating pile", *Tunnelling and Underground Space Technology*, 86, 138-155, https://doi.org/10.1016/j.tust.2019.01.012.

Soomro, M.A., Mangi, N., Cheng, W. and Mangnejo, A. (2020). "The effects of multipropped deep excavation-induced ground movements on adjacent high-rise building founded on piled raft in sand", *Advances in Civil Engineering*, 2020(1), 8897507, https://doi.org/10.1155/2020/8897507.

Teh, K.L., Leung, C.F. and Chow, Y.K. (2005). "Spud can penetration in sand overlying clay", *Soil Mechanics | Geotechnical Engineering*, ISFOG 2005, Perth, Australia, 529-534, https://scholarbank.nus.edu.sg/handle/10635/74363.

Ünsever, Y.S. (2015). "An experimental study on static and dynamic behaviour of model pile foundations", Ph.D. Thesis, Middle East Technical University, Turkey, https://open.metu.edu.tr/bitstream/handle/11511/24493/index.pdf.

Yi, S. (2022). "Parametric study of passive piles subjected to adjacent surcharge load in extensively deep soft soil", *Frontiers in Materials*, 9, 1080547, http://doi.org/10.3389/fmats.2022.1080547.

Zhang, R., Zhang, W. and Goh, A.T. (2018). "Numerical investigation of pile responses caused by adjacent braced excavation in soft clays", *International Journal of Geotechnical Engineering*, 15(7), 783-797, https://doi.org/10.1080/19386362.2018.1515810.